J Mater Sci: Mater Med (2011) 22:753–761
DOI 10.1007/s10856-011-4251-5

# In vitro dissolution and corrosion study of calcium phosphate coatings elaborated by pulsed electrodeposition current on Ti6Al4V substrate

**R. Drevet · F. Velard · S. Potiron · D. Laurent-Maquin · H. Benhayoune**

Received: 23 November 2010 / Accepted: 23 January 2011 / Published online: 3 February 2011


**Abstract** Calcium-deficient hydroxyapatite (Ca-def-HAP) coatings on titanium alloy (Ti6Al4V) substrates are elaborated by pulsed electrodeposition. In vitro dissolution/precipitation process is investigated by immersion of the coated substrate into Dulbecco's Modified Eagle Medium (DMEM) from 1 h to 28 days. Calcium and phosphorus concentrations evolution in the biological liquid are determined by Induced Coupled Plasma-Atomic Emission Spectroscopy (ICP-AES) for each immersion time. Physical and chemical characterizations of the coating are performed by scanning electron microscopy (SEM) associated to Energy Dispersive X-ray Spectroscopy (EDXS) for X-ray microanalysis. Surface modifications are investigated by an original method based on the three-dimensional reconstruction of SEM images (3D-SEM). Moreover, corrosion measurements are carried out by potentiodynamic polarization experiments. The results show that the precipitation rate of the Ca-def HAP coating is more pronounced in comparison with that of stoichiometric hydroxyapatite (HAP) used as reference. The precipitated bone-like apatite coating is thick, homogenous and exhibits an improved link to the substrate. Consequently, the corrosion behaviour of the elaborated prosthetic material is improved.

R. Drevet (✉) · F. Velard · S. Potiron · D. Laurent-Maquin · H. Benhayoune
INSERM UMR-S 926, IFR 53, URCA, 21 rue Clément Ader, BP 138, 51685 Reims Cedex 02, France
e-mail: richard.drevet@univ-reims.fr

## 1 Introduction

Titanium and its alloys are widely used as implant materials in orthopaedic surgery because of their good biocompatibility with bone. However, a way to make them bioactive is to coat them with calcium phosphate ceramics which are able to form a real bond with the surrounding bone tissue in vivo [1–4]. Many methods are developed and used to prepare calcium phosphate coatings onto implant surfaces, for example, plasma spray [5–7], sol–gel [8–10], pulsed laser-deposition [11, 12], electrophoretic method [13–15] and electrochemical deposition [16–20]. This last method has a variety of advantages compared to other methods and especially to plasma spray which is the actual industrial standard method: the coating process occurs at low temperature, the thickness and the chemical composition are controlled.

However, when using high current density, a large amount of $H_2$ bubbles is produced at the vicinity of the cathode leading to non uniform and weakly adherent coatings [21]. In order to solve these problems, pulsed electrodeposition may be used [22]. Indeed, the use of a relaxation time between two deposition times (pulse cycle) strongly reduces $H_2$ bubbles emission allowing the calcium phosphate coating to be adequately deposited.

When calcium phosphates are immersed into biological medium, they are subject to a dissolution process immediately followed by the precipitation of a bone-like apatite phase that point out the bioactivity of the prosthetic material [23]. This process modifies the surface morphology and the thickness of the coating. The present investigation follows, as a function of immersion time, the dissolution/precipitation and corrosion processes into Dulbecco's Modified Eagle Medium (DMEM) of a calcium phosphate coating elaborated by pulsed electrodeposition.

The results are systematically compared to those obtained for stoichiometric hydroxyapatite used as a reference since its behaviour in biological solution is well established. Moreover, the surface modification of the coating as a function of immersion time is also studied.

## 2 Experimental

### 2.1 Electrodeposition

Figure 1a represents schematically the experimental setup of the electrolytic cell used for calcium phosphate coatings electrodeposition as described previously [24]. The electrolyte was prepared by dissolving 0.042 M $Ca(NO_3)_2$ $4H_2O$ and 0.025 M $NH_4(H_2PO_4)$ in ultra-pure water. The measured pH value was 4.4 and the temperature fixed at 60°C.

The Ti6Al4V substrates were disks of 12 mm diameter and 4 mm thickness. Prior to coating, they were etched in a mixture of acids consisting of nitric acid ($HNO_3$, 6% in volume) and hydrofluoric acid (HF, 3% in volume). Then, they were ultrasonically cleaned in acetone and in ultra-pure water. Electrodeposition was performed by pulsing the current as indicated in Fig. 1b. A cycle is composed of a time deposition $t_d = 1$ min with a current density $j_d = -15$ mA cm$^{-2}$ followed by a break time $t_b = 2$ min ($j_b = 0$ mA cm$^{-2}$). The number of deposition cycles was fixed to five which correspond to a total deposition time of 15 min.

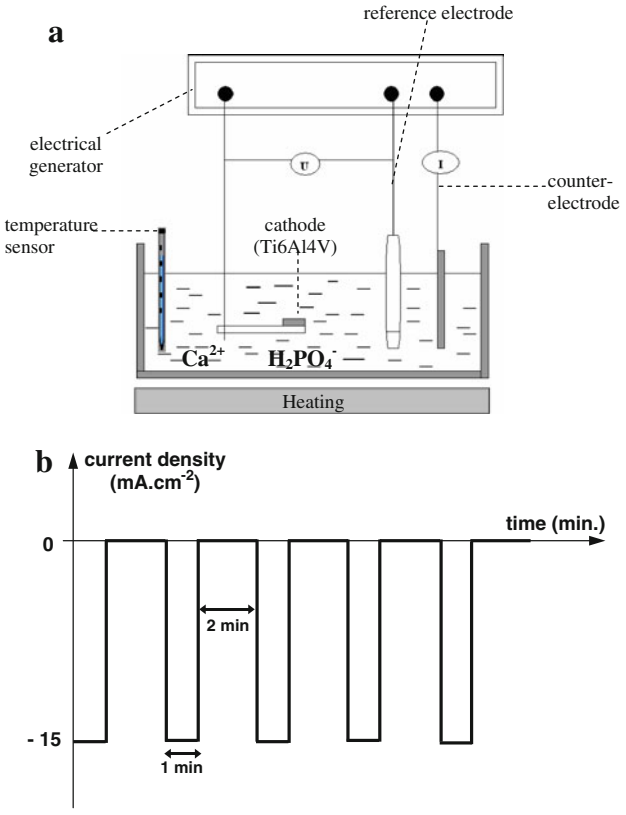


**Fig. 1** Principle of pulsed electrodeposition current: **a** schematic view of the experimental set-up and **b** pulsed current evolution as a function of time

After electrodeposition the specimens were dried and annealed at 550°C during 2 h in order to stabilize the coatings and to improve their adhesion to the substrates [24].

The stoichiometric hydroxyapatite (HAP) coatings used as reference for dissolution studies were obtained by using the same electrodeposition procedure associated with 9% of hydrogen peroxide into electrolyte as we described in a recent work [25].

### 2.2 Scanning electron microscopy and X-ray analysis

The coatings morphologies and the coating/substrate cross-sections were observed using a LaB6 electron microscope (JEOL JSM-5400LV) operating at 0–30 kV. This microscope is associated to an ultra-thin window Si(Li) detector for X-ray measurements (GENESIS, Eloïse SARL, France). The specimens are coated with a conductive layer (Au–Pd for SEM micrographs and carbon for X-ray microanalysis). The X-ray spectra were acquired at primary beam energy of 15 kV with an acquisition time of 100 s. For the quantitative analysis (concentration and thickness), commercial software (GENESIS, Eloïse SARL, France) associated with an original procedure for coating analysis developed in our laboratory is used [26–28]. Several measurements were carried out to calculate a mean value of Ca/P atomic ratio and coating thickness $t$ with standard deviation.

X-ray maps (256 × 200 pixels) of the coatings surface were obtained by scanning a 68 µm × 54 µm area with 0.05 s per pixel time (which corresponded to a total acquisition time of about 45 min).

3D reconstruction of the coating surfaces was carried out using commercial software (MeX, Alicona, France). This method consists in a combination of stereoscopic images obtained by inclination of the sample in SEM. Therefore, digital elevation model (DEM) and roughness profiles of the surface specimen are obtained.

### 2.3 Scanning transmission electron microscopy (STEM)

A Philips CM30 operating from 100 to 300 kV was used to study the morphology of the samples at a nanometre level. The cross-sections were prepared using a specific method developed in our laboratory and previously described [25].

**Table 1** Chemical composition of DMEM

| Components | Concentration (g $l^{-1}$) |
|---|---|
| Inorganic salts | |
| NaCl | 6.400 |
| $NaHCO_3$ | 3.700 |
| KCl | 0.400 |
| $CaCl_2$ | 0.264 |
| $MgSO_4 \cdot 7H_2O$ | 0.200 |
| $NaH_2PO_4 \cdot H_2O$ | 0.125 |
| Other components | |
| Amino acids | 1.843 |
| Vitamins | 0.032 |
| Glucose | 4.500 |
| Sodium pyruvate | 0.110 |
| Phenol red Na | 0.016 |

### 2.4 X-ray diffraction analysis

For the phase composition investigation, powder was scratched from the coating and analysed with an X-ray diffractometer Bruker D8 Advance. The X-ray pattern data were collected from $2\theta = 10°$ to 45° using a monochromatic CuKα radiation at the step of 0.04 degrees with a count time of 12 s at each step. The calcium phosphate structures were identified basing on JCPDS files and the percentage of crystallinity was determined following standard ISO 13779-3 [29].

### 2.5 Dissolution experiments

The electrodeposited coatings were immersed in triplicate in 7 ml of Dulbecco's Modified Eagle Medium: DMEM

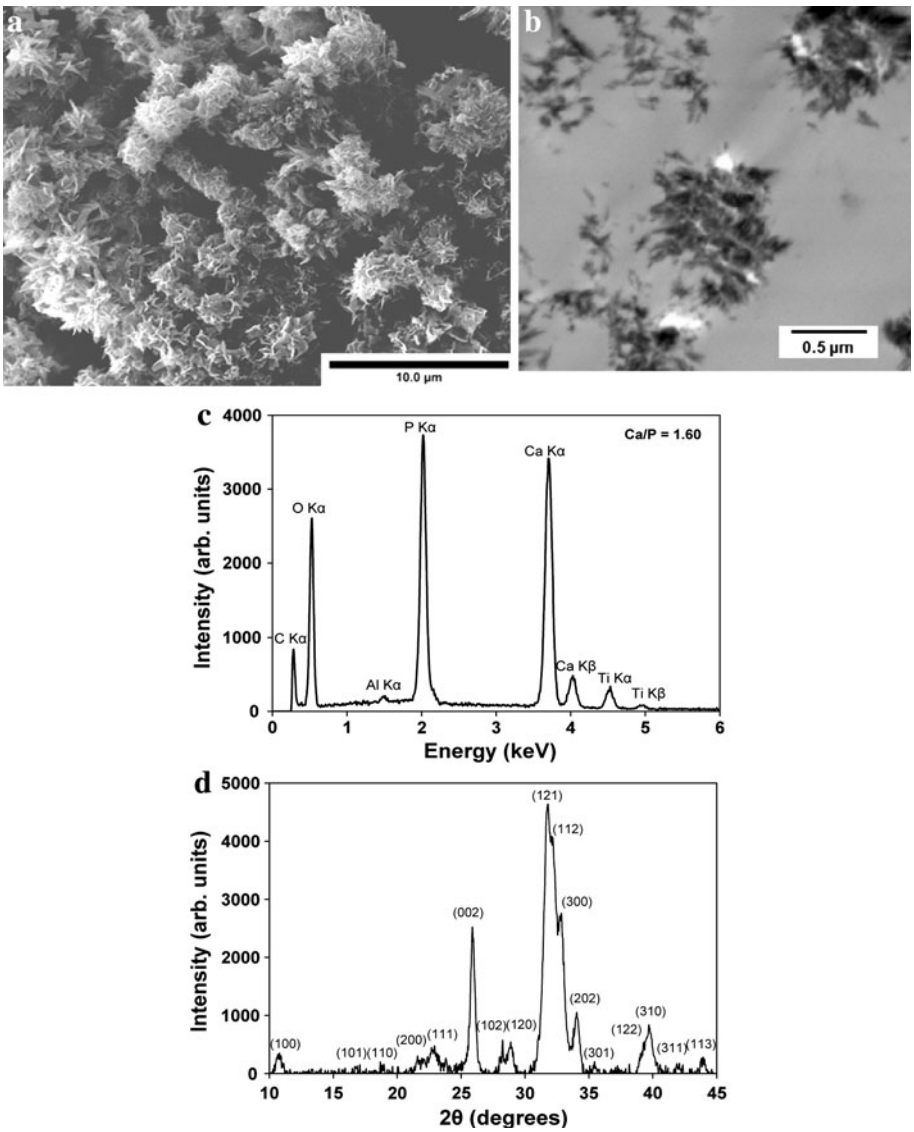


**Fig. 2** Characterization of the electrodeposited coating: **a** SEM and **b** STEM micrographs, **c** EDXS spectrum and **d** XRD pattern

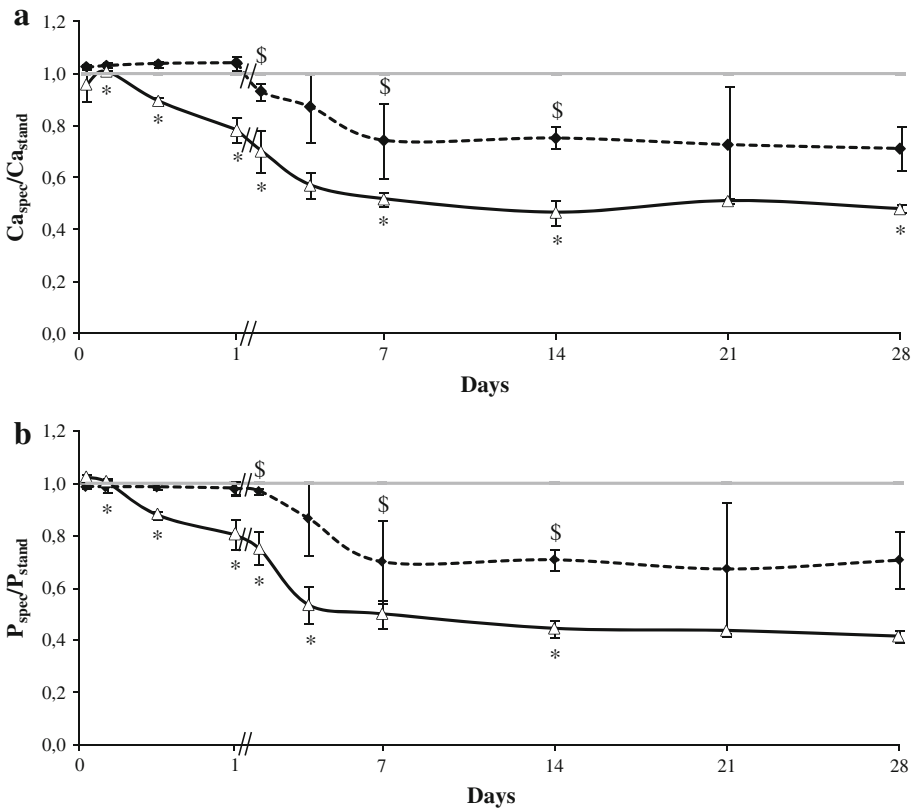


**Fig. 3** $\left(\frac{Ca_{spec}}{Ca_{stand}}\right)$ **a** and $\left(\frac{P_{spec}}{P_{stand}}\right)$ **b** ratios measured by ICP-AES as a function of immersion time in DMEM. Shown are the mean values of nine measures ± SD. *Gray solid line* represents DMEM alone as reference, *black dashed line* and *black solid line* represent HAP standard coating and Ca-def HAP coating respectively. $ and * mean $P < 0.05$ compared to the previous time value for HAP standard coating and Ca-def HAP coating respectively

(Table 1) at 37°C in humidified atmosphere containing 5% $CO_2$. The different incubation periods tested were 1, 4 and 12 h and 1, 2, 4, 7, 14, 21 and 28 days. After these immersion times, the specimens were retrieved, rinsed by dipping in distilled water and then dried and kept at 37°C for SEM analysis and the media were collected to determine the Ca and P amounts using ICP-AES (Induced Coupled Plasma–Atomic Emission Spectroscopy, VARIAN Liberty Série II). Measurements were performed in triplicate. The measured values were systematically compared to those of HAP coating (reference) measured in the same experimental conditions.

### 2.6 Statistical analysis

Significance of data obtained from ICP-AES experiments was assessed using a non parametric Mann & Whitney Test (StatXact 7.0, Cytel Inc, Cambridge, MA, USA). Difference between two conditions was considered significant when $P < 0.05$.

### 2.7 In vitro electrochemical corrosion studies

Potentiodynamic polarization experiments were used to evaluate the corrosion behaviour of electrodeposited coatings on Ti6Al4V before and after immersion into DMEM. The temperature was maintained at 37°C. The polarization curves (potential variation as a function of current density) were determined by increasing the potential at a scan rate of 1.0 mV $s^{-1}$. Measurements were performed in triplicate.

## 3 Results

The SEM micrograph of the electrodeposited coating shown in Fig. 2a indicates that the coating is composed of small needles and crystallites. The Scanning transmission electron microscopy (STEM) micrograph of Fig. 2b confirms these observations and shows that the needles size is less than 0.2 μm. Quantitative analysis from X-ray spectrum of Fig. 2c give a Ca/P atomic ratio of 1.60 ± 0.02 and a thickness $t = 7.9 \pm 0.6$ μm. XRD pattern of Fig. 2d shows that the coating is composed of an apatitic phase of low crystallinity with typical diffraction peaks at $2\theta = 25.9°–31.8°–32.2°–32.9°–34°–39.8°$ corresponding to hydroxyapatite (JCPDS 09-0432). The calculated percentage of crystallinity was 65%. The combination of Scanning electron microscopy and X-ray analysis (SEM-EDXS) and XRD results indicates that the obtained coating corresponds to a calcium deficient hydroxyapatite (Ca-def HAP) [30].

Next, these coatings were immersed in DMEM until 28 days. In order to show the evolution of calcium and phosphorus concentration in DMEM collected after each

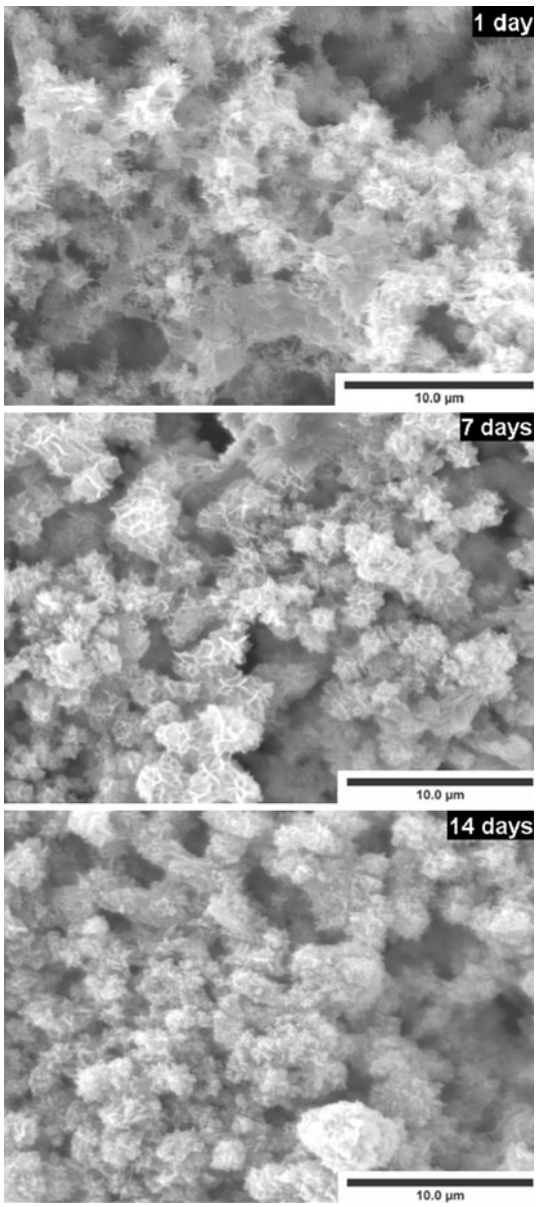


**Fig. 4** SEM micrographs of the coating showing the modification of the morphology after 1, 7 and 14 days of immersion time in DMEM

time period, we determined by ICP-AES the ratios $Ca_{spec}/Ca_{stand}$ and $P_{spec}/P_{stand}$.

The $Ca_{spec}$ and $P_{spec}$ (specimen) are respectively, the measured calcium and phosphorus concentrations in DMEM which were in contact with the coatings.

The $Ca_{stand}$ and $P_{stand}$ (standard) are respectively, the calcium and phosphorus concentrations in DMEM alone measured in the same experimental conditions.

The obtained results are presented in Fig. 3. For the HAP coating (reference), the data demonstrated that $Ca_{spec}/Ca_{stand}$ (Fig. 3a) and $P_{spec}/P_{stand}$ (Fig. 3b) ratios do not exhibit any variations ($P > 0.05$) before 2 days of immersion. Then, significant 21 and 27% decreases ($P < 0.05$) are observed from 2 to 14 days of immersion (for $Ca_{spec}/Ca_{stand}$ and $P_{spec}/P_{stand}$ ratios respectively) which stabilized thereafter ($P > 0.05$). Concerning the Ca-def HAP coating, the results highlight a significant decrease from 4 h to 14 days of immersion for both elements (48 and 50% respectively for $Ca_{spec}/Ca_{stand}$ and $P_{spec}/P_{stand}$ ratios). Finally, the values reached a plateau until 28 days of immersion in DMEM. Based on ICP-AES results, we focused the SEM characterizations of the immersed specimens on the main delays 1, 7 and 14 days. The results are presented on Fig. 4. One may observe a progressive change of the coating morphology especially after 14 days of immersion where the precipitated coating is homogenous and less porous than 1 day sample. The SEM cross-sections of Fig. 5 show that the precipitated coating thickness is enhanced reaching about 35 µm with an improved link to the substrate. These observations are confirmed by elemental X-ray maps of Fig. 6 showing that calcium and phosphorus distributions are more homogenous from 1 to 14 days compared to those of non-immersed coating. Moreover, the X-ray intensity of titanium substrate decreases significantly, mainly at 7 and 14 days which confirms the important thickness increase of the precipitated coating.

On the other hand, to illustrate the decrease of the porosity, 3D-SEM reconstructions were carried out. Figure 7 shows topographic images of the samples from 0 to 14 days of immersion. The corresponding profiles (Fig. 8) clearly indicate an important reduction of depth/height differences. The corresponding roughness values presented in Table 2 underline the decrease observed as a function of immersion time. For example, the arithmetic roughness (Ra) of the coating decreases from 4.9 µm before immersion to 2.9 µm after 14 days of immersion.

Furthermore we hypothesized that Ca-def HAP coatings modifications can alter corrosion properties of the samples. Figure 9 shows polarization curves of the uncoated Ti6Al4V (a) compared to Ca-def HAP/Ti6Al4V at 0 day (b) and 7 days (c) of immersion. A shift to nobler values can clearly be observed for coated Ti6Al4V samples. The corrosion potential value increased from −0.514 V for the uncoated Ti6Al4V to −0.394 V for the Ca-def HAP/Ti6Al4V sample. After 7 days of immersion, the corrosion potential reaches 0.104 V indicating that the pulsed electrodeposited coating acts as a protective barrier for the titanium substrate and improves its corrosion protection in biological liquid.

## 4 Discussion

In this work we have elaborated and characterized a suitable biomaterial for titanium alloy prosthesis coating. Its bioactivity is greater than one of HAP, the gold standard material in the field [31].

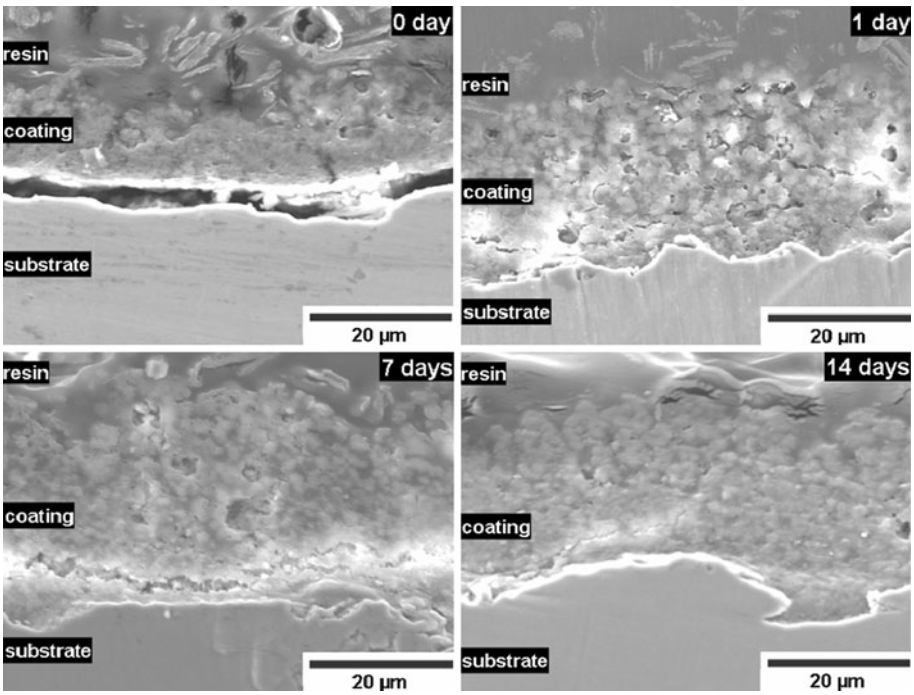


**Fig. 5** Cross-section SEM micrographs showing the thickness and the coating/substrate interface evolutions before and after 1, 7 and 14 days of immersion time in DMEM

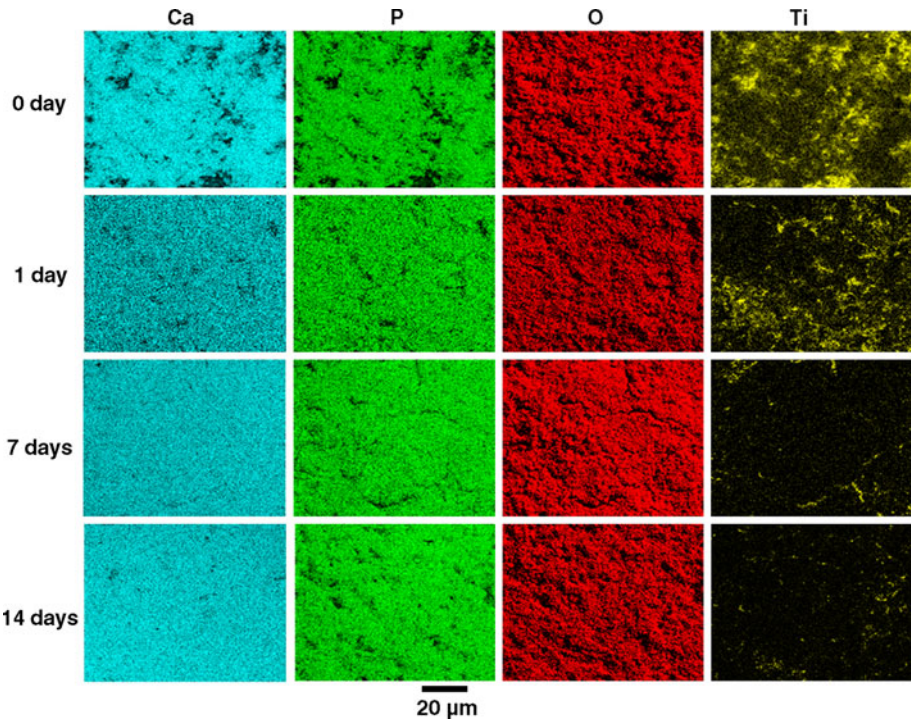


**Fig. 6** EDXS elemental maps of the coating as a function of immersion time in DMEM

We have performed biomaterial synthesis using pulsed electrodeposition of calcium phosphate to avoid the problems linked to $H_2$ bubbles generation at the Ti6Al4V cathode [24]. When the current density is applied, reduction of water occurs at the cathode as:

$$2H_2O + 2e^- \rightarrow H_2 + 2OH^- \quad (1)$$

Then, the pH at the vicinity of the cathode increases, therefore reaction (1) is followed by acid–base reactions of phosphate ions such as:

$$H_2PO_4^- + OH^- \rightarrow HPO_4^{2-} + H_2O \quad (2)$$

$$HPO_4^{2-} + OH^- \rightarrow PO_4^{3-} + H_2O \quad (3)$$

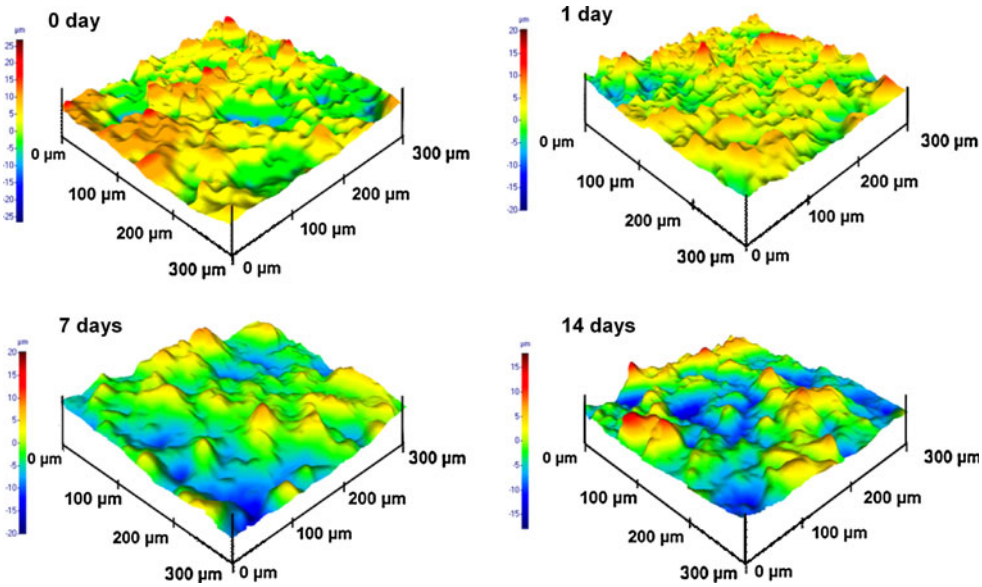


**Fig. 7** 3D-SEM reconstruction of the coating surface before and after 1, 7 and 14 days of immersion time in DMEM

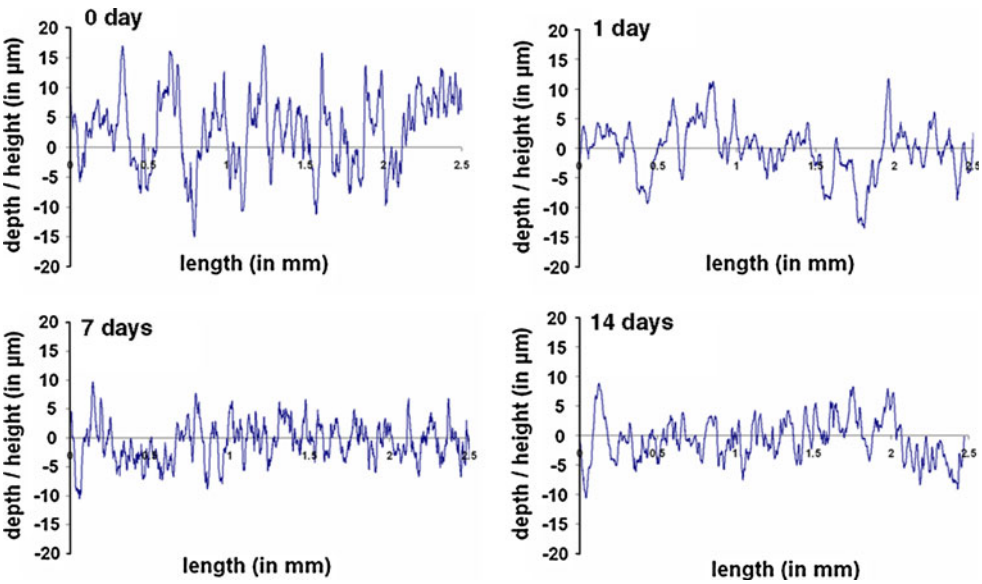


**Fig. 8** Roughness profile of the coating before and after 1, 7 and 14 days of immersion time in DMEM

**Table 2** Roughness parameters of the calcium phosphate coating surface as a function immersion time in DMEM

| | 0 day | 1 day | 7 days | 14 days |
|---|---|---|---|---|
| Ra (µm) | 4.9 | 3.5 | 2.8 | 2.9 |
| RMS (µm) | 6.0 | 4.7 | 3.4 | 3.5 |
| Rz (µm) | 31.9 | 24.9 | 19.9 | 18.8 |

*Ra* arithmetic roughness, *RMS* root-mean square roughness, *Rz* maximum height of roughness profile

At these pH values (more than 13), the minority specie is $HPO_4^{2-}$ and the predominant specie is $PO_4^{3-}$ as shown by Eliaz et al. [32]. Therefore, calcium deficient hydroxyapatite (Ca-def HAP) phase precipitates as:

$$9.5\,Ca^{2+} + 5.5\,PO_4^{3-} + 0.5\,HPO_4^{2-} + 0.5\,OH^- \rightarrow Ca_{9.5}(HPO_4)_{0.5}(PO_4)_{5.5}(OH)_{0.5} \quad (4)$$

Indeed, the SEM-EDXS and XRD characterizations of the biomaterial have highlighted a calcium-deficient hydroxyapatite (Ca-def HAP). To investigate on this coating's bioactivity in biological fluid, we performed immersion experiments followed by morphological examinations of the samples to show their surface modifications. In fact, as it is well described [33], the calcium phosphate coating is dissolved initially releasing $Ca^{2+}$ and $PO_4^{3-}$ ions into the solution. With increasing the ions concentrations, the solution becomes super-saturated with those ions resulting in a re-precipitation of apatite. The precipitation rate in the case of Ca-def HAP is more

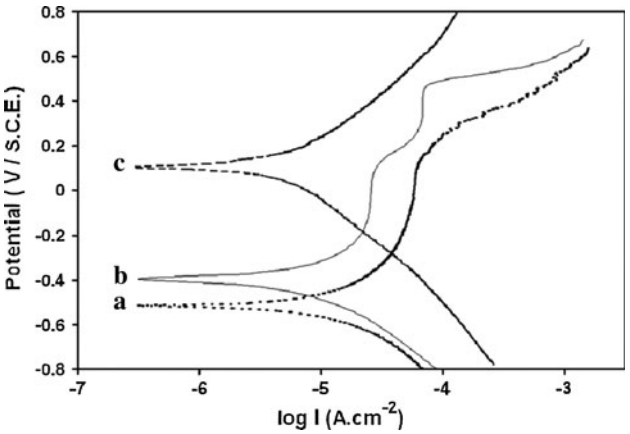


**Fig. 9** Polarization curves of **a** uncoated Ti6Al4V substrate, **b** as-deposited Ca-def HAP coating and **c** Ca-def HAP coating after 7 days of immersion in DMEM

pronounced than that of HAP (reference). For example, the $Ca_{spec}/Ca_{stand}$ ratio passed from 1 at 0 day to 0.48 at 28 days in the case of Ca-def HAP and only to 0.7 in the case of HAP. The precipitation process is more rapid in the case of Ca-def HAP than in HAP. The $Ca_{spec}/Ca_{stand}$ ratio of Ca-def HAP reached the 0.7 value through 2 days compared to 28 days for HAP.

The dissolution/precipitation process of the coating was also illustrated across the morphological changes observed by SEM, especially the improvement of the bond between the titanium alloy substrate and the Ca-def HAP coating as it is a critical parameter in coated-implant lifespan [34]. In addition, the increase of the coating's thickness and the decrease of its roughness observed by SEM cross-sections and X-ray elemental maps play an important role on its corrosion behaviour as confirmed by polarization measurements.

## 5 Conclusion

In this work, the bioactivity of a Ca-def HAP coating on titanium alloy elaborated by pulsed electrodeposition was investigated. It is demonstrated that the dissolution/precipitation process into biological liquid (DMEM) is more pronounced in comparison with stoichiometric HAP coating used as reference. The characterization of the precipitated coating exhibited a compact and thick coating leading to an improvement of its corrosion protection in biological liquid. We believe that this biomaterial will be considered as an alternative to the stoichiometric HAP usually employed in implant industry.

## References

1. Rammelt S, Heck C, Bernhardt R, Bierbaum S, Scharnweber D, Goebbels J, et al. In vivo effects of coating loaded and unloaded Ti implants with collagen, chondroitin sulfate, and hydroxyapatite in the sheep tibia. J Orthop Res. 2007;25:1052–61.
2. Yildirim OS, Aksakal B, Hanyaloglu SC, Erdogan F, Okur A. Hydroxyapatite dip coated and uncoated titanium poly-axial pedicle screws: an in vivo bovine model. Spine. 2006;31:1780–8.
3. Schouten C, Meijer GJ, Van den Beucken JJJP, Leeuwenburgh SCG, De Jonge LT, Wolke JGC, et al. In vivo bone response and mechanical evaluation of electrosprayed CaP nanoparticle coatings using the iliac crest of goats as an implantation model. Acta Biomater. 2010;6:2227–36.
4. Borsari V, Fini M, Giavaresi G, Tschon M, Chiesa R, Chiusoli L, et al. Comparative in vivo evaluation of porous and dense duplex titanium and hydroxyapatite coating with high roughnesses in different implantation environments. J Biomed Mater Res A. 2009;89:550–60.
5. Hesse C, Hengst M, Kleeberg R, Götze J. Influence of experimental parameters on spatial phase distribution in as-sprayed and incubated hydroxyapatite coatings. J Mater Sci Mater Med. 2008;19:3235–41.
6. Lombardi AVJ, Berend KR, Mallory TH. Hydroxyapatite-coated titanium porous plasma spray tapered stem—experience at 15 to 18 years. Clin Orthop Relat Res. 2006;453:81–5.
7. Chen CC, Huang TH, Kao CT, Ding SJ. Characterization of functionally graded hydroxyapatite/titanium composite coatings plasma-sprayed on Ti alloys. J Biomed Mater Res B Appl Biomater. 2006;78B:146–52.
8. Eshtiagh-Hosseini H, Housaindokht M, Chahkandi M. Effects of parameters of sol–gel process on the phase evolution of sol–gel-derived hydroxyapatite. Mater Chem Phys. 2007;106:310–6.
9. Fellah BH, Layrolle P. Sol–gel synthesis and characterization of macroporous calcium phosphate bioceramics containing microporosity. Acta Biomater. 2009;5:735–42.
10. Wang D, Chen C, He T, Lei T. Hydroxyapatite coating on Ti6Al4V alloy by a sol–gel method. J Mater Sci Mater Med. 2008;19:2281–6.
11. Kim H, Camata RP, Lee S, Rohrer GS, Rollett AD, Vohra YK. Crystallographic texture in pulsed laser deposited hydroxyapatite bioceramic coatings. Acta Mater. 2007;55:131–9.
12. Dinda GP, Shin J, Mazumder J. Pulsed laser deposition of hydroxyapatite thin films on Ti–6Al–4V: effect of heat treatment on structure and properties. Acta Biomat. 2009;5:1821–30.
13. Yamaguchi S, Yabutsuka T, Hibino M, Yao T. Generation of hydroxyapatite patterns by electrophoretic deposition. J Mater Sci Mater Med. 2008;19:1419–24.
14. Corni I, Ryan MP, Boccaccini AR. Electrophoretic deposition: from traditional ceramics to nanotechnology. J Europ Ceram Soc. 2008;28:1353–67.
15. Kwok CT, Wong PK, Cheng FT, Man HC. Characterization and corrosion behavior of hydroxyapatite coatings on Ti6Al4V fabricated by electrophoretic deposition. Appl Surf Sci. 2009;255:6736–44.
16. Benhayoune H, Laquerriere P, Jallot E, Perchet A, Kilian L, Balossier G, et al. Micrometer level structural and chemical evaluation of electrodeposited calcium phosphate coatings on TA6V substrate by STEM-EDXS. J Mater Sci Mater Med. 2002;13:1057–63.
17. Eliaz N, Eliyahu M. Electrochemical processes of nucleation and growth of hydroxyapatite on titanium supported by real-time electrochemical atomic force microscopy. J Biomed Mater Res A. 2007;80:621–34.
18. Abdel-Aal EA, Dietrich D, Steinhaeuser S, Wielage B. Electrocrystallization of nanocrystallite calcium phosphate coatings on titanium substrate at different current densities. Surf Coat Tech. 2008;202:5895–900.

19. Kuo MC, Yen SK. The process of electrochemical deposited hydroxyapatite coatings on biomedical titanium at room temperature. Mater Sci Eng C. 2002;20:153–60.
20. Lopez-Heredia MA, Weiss P, Layrolle P. An electrodeposition method of calcium phosphate coatings on titanium alloy. J Mater Sci Mater Med. 2007;18:381–90.
21. Wang SH, Shih WJ, Li WL, Hon MH, Wang MC. Morphology of calcium phosphate coatings deposited on a Ti–6Al–4V substrate by an electrolytic method under 80 Torr. J Europ Ceram Soc. 2005;25:3287–92.
22. Lin S, LeGeros RZ, LeGeros JP. Adherent octacalciumphosphate coating on titanium alloy using modulated electrochemical deposition method. J Biomed Mater Res A. 2003;66:819–28.
23. Zhang Q, Chen J, Feng J, Cao Y, Deng C, Zhang X. Dissolution and mineralization behaviours of HA coatings. Biomaterials. 2003;24:4741–8.
24. Benhayoune H, Drevet R, Faure J, Potiron S, Gloriant T, Oudadesse H, et al. Elaboration of monophasic and biphasic calcium phosphate coatings on Ti6Al4V substrate by pulsed electrodeposition current. Adv Eng Mater. 2010;12(6):B192–9.
25. Drevet R, Benhayoune H, Wortham L, Potiron S, Douglade J, Laurent-Maquin D. Effects of pulsed current and $H_2O_2$ amount on the composition of electrodeposited calcium phosphate coatings. Mater Charact. 2010;61:786–95.
26. Dumelie N, Benhayoune H, Balossier G. TF_Quantif: a procedure for quantitative mapping of thin films on heterogeneous substrates in electron probe microanalysis (EPMA). J Phys D Appl Phys. 2007;40:2124–31.
27. Benhayoune H. X-ray microanalysis of multi-elements coatings using Auger formalism: application to biomaterials. J Phys D Appl Phys. 2002;35:1526–31.
28. Benhayoune H, Dumelie N, Balossier G. Substrate effects correction in Auger spectroscopy and electron probe microanalysis of thin films. Thin Solid Films. 2005;493:113–23.
29. ISO 13779-3. Implants for surgery—hydroxyapatite—part 3: chemical analysis and characterization of crystallinity and phase purity.
30. Dumelie N, Benhayoune H, Rousse-Bertrand C, Bouthors S, Perchet A, Wortham L, et al. Characterization of electrodeposited calcium phosphate coatings by complementary scanning electron microscopy and scanning-transmission electron microscopy associated to X-ray microanalysis. Thin Solid Films. 2005;492:131–9.
31. LeGeros RZ. Calcium phosphate-based osteoinductive materials. Chem Rev. 2008;108:4742–53.
32. Eliaz N, Sridhar TM. Electrocrystallization of hydroxyapatite and its dependence on solution conditions. Cryst Growth Des. 2008;8:3965–77.
33. Dumelie N, Benhayoune H, Richard D, Laurent-Maquin D, Balossier G. In vitro precipitation of electrodeposited calcium-deficient hydroxyapatite coatings on Ti6Al4V substrate. Mater Charact. 2008;59:129–33.
34. Paital SR, Dahotre NB. Calcium phosphate coatings for bio-implant applications: materials, performance factors, and methodologies. Mater Sci Eng R. 2009;66:1–70.